# Solvation Effects in SINDO1: Application to Organic Molecules

**CHRISTIAN KÖLLE AND KARL JUG***

*Theoretische Chemie, Universität Hannover, Am Kleinen Felde 30, 30167 Hannover, Germany*

*Received 23 August 1995; accepted 2 January 1996*

**ABSTRACT**

The polarizable continuum model of Miertus et al. was implemented in the semiempirical molecular orbital method SINDO1. A fast and precise method for the calculation of solvation energies is achieved based on isodensity surfaces for the cavity surface and on approximated electrostatic potentials. The calculated solvation energies in water agree well with experimental and other calculated data. © 1997 by John Wiley & Sons, Inc.

## Introduction

The theoretical description of solution effects with continuum models has received increased attention in recent years. Tomasi and Persico[1] reviewed the development in this field. Besides Monte Carlo[2,3] and molecular dynamics[4] methods, continuum models are the most important methods for the description of the interaction of solute and solvent molecules. Applications comprise the calculation of solvation energies,[5–10] the influence of the solvent on the conformation of organic molecules,[11–13] the calculation of electronic spectra in solution,[14–17] and more recently chemical reactions in solution.[18,19]

In continuum models the solvent is considered as a homogeneous dielectric. Therefore, only macroscopic properties of the solvent are used in the calculations. The solute molecule is located in a cavity in the dielectric. The various continuum models are distinguished by the form of these cavities and by the representation of the charge distribution of the solute molecule. For spheres and ellipsoids as cavities and a multipole expansion for the charge distribution, the electrostatic equations can be solved analytically.[20] The procedures of Rinaldi and Rivail,[21] Tapia and Goscinski,[22] and Wong et al.[23] are based on these simplifying assumptions. The use of more realistic cavities forces us to solve the electrostatic problem numerically. The polarizable continuum model (PCM) of Miertus and colleagues[24] is a procedure that uses such a numerical solution. Although originally developed for *ab initio* methods, the PCM has recently been introduced to semiempirical methods.[7,25,26] In the present work we present the implementation of the PCM into the SINDO1 method[27–29] in combination with the asymptotic density model (ADM)[30] for the molecular electrostatic potential (MESP). The latter provides a significant reduction of the computer time for the

* Author to whom all correspondence should be addressed.


© 1997 by John Wiley & Sons
CCC 0192-8651 / 97 / 010001-08

MESP while retaining the quality of the MESP, resulting in an accurate calculation of the electrostatic interaction. As a new idea in this context we use isodensity surfaces for the calculation of the cavity surfaces because they provide a physical description of molecular surfaces.[13]

## Solvation Model in SINDO1

In the PCM[24] the solvent is considered as an infinitely extended, homogeneous, polarizable dielectric with the dielectric constant $\varepsilon$. The solute molecule is located in a cavity in this dielectric. The charge distribution of the solute molecule generates an electric field that polarizes the dielectric. The polarization of the dielectric induces a field that in turn has an effect on the solute molecule. This induced field is called the reaction field. The effect of the reaction field on the solute molecule is described by a perturbation $\hat{V}_R$ of the Hamiltonian operator $\hat{H}^{(0)}$ of the vacuum system.

$$\left(\hat{H}^{(0)} + \hat{V}_R\right)\Psi = E\Psi. \tag{1}$$

The reaction field is described in the PCM by a virtual surface charge distribution $\sigma(\mathbf{s})$ on the cavity surface $S$,

$$V_R(\mathbf{r}) = \int_S \frac{\sigma(\mathbf{s})}{|\mathbf{r} - \mathbf{s}|}\, d\mathbf{s}. \tag{2}$$

For the numerical calculation of $\sigma(\mathbf{s})$ the surface $S$ is subdivided in segments $i$ and each segment is assigned a charge $q_i$,

$$V_R(\mathbf{r}) = \sum_{i=1}^{M} \frac{\sigma(\mathbf{s}_i)S_i}{|\mathbf{r} - \mathbf{s}_i|} = \sum_{i=1}^{M} \frac{q_i}{|\mathbf{r} - \mathbf{s}_i|}. \tag{3}$$

Here $m$ is the number of surface segments, $S_i$ the size of the surface $i$, and $q_i$ the charge of the surface segment $i$. The vectors $\mathbf{r}$, $\mathbf{s}$, and $\mathbf{s}_i$ are illustrated in Figure 1. The charge distribution $\sigma(\mathbf{s}_i)$ is calculated via the solution of the Laplace equation,[24]

$$\sigma(\mathbf{s}_i) = -\frac{\varepsilon - 1}{4\pi\varepsilon}\left(\frac{\partial V_T(\mathbf{s}_i)}{\partial \mathbf{n}_i}\right). \tag{4}$$

$\mathbf{n}_i$ is the normal vector of the surface for point $\mathbf{s}_i$. $V_T(\mathbf{s}_i)$ is the total electrostatic potential of the solute molecule consisting of the electrostatic potential of the solute molecule $V_M(\mathbf{s}_i)$ and the surface charge generated potential $V_R(\mathbf{s}_i)$,

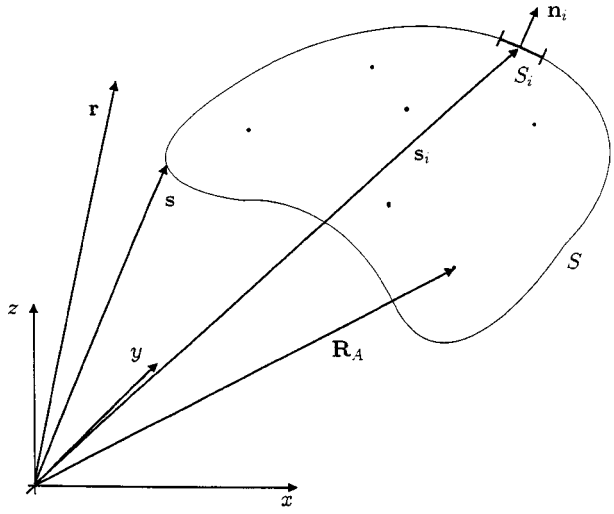


**FIGURE 1.** Definition of vectors $\mathbf{r}$, $\mathbf{s}$, and $\mathbf{s}_i$.

$$V_T(\mathbf{s}_i) = V_M(\mathbf{s}_i) + V_R(\mathbf{s}_i). \tag{5}$$

Because the virtual surface distribution $\sigma(\mathbf{s}_i)$ is adjusted in a self-consistent way, $V_R(\mathbf{r})$ is also determined in an iterative process using eqs. (5), (4), and (3). The iteration process is initiated with a $V_T(\mathbf{s}_i)$ where the reaction field contribution $V_R(\mathbf{s}_i)$ is neglected.

The PCM was implemented in this form in SINDO1. The latter method[27–29] is based on the INDO approximation in a minimal basis set of Slater orbitals. The error due to the neglect of the differential overlap is reduced by the symmetric orthogonalization. We shall come back later to the calculation of the cavity surface $S$ and the electrostatic potential $V_M(\mathbf{s}_i)$.

The electrostatic free solvation energy can be formulated in the PCM as[6]

$$\Delta G_{\text{el}} = E - E^0 - \tfrac{1}{2}\langle\Psi|\hat{V}_R|\Psi\rangle, \tag{6}$$

where $E$ is the energy in solution and $E^0$ is the energy in vacuum. $E - E^0$ is the energy released if the molecule is brought into the cavity inside the polarized dielectric. The third term on the right side of (6) is the necessary energy for the polarization of the dielectric.[5] The total free solvation energy $\Delta G_{\text{sol}}$ consists of $\Delta G_{\text{el}}$ and further parts like the dispersion energy $\Delta G_{\text{dis}}$, the repulsion energy $\Delta G_{\text{rep}}$, and the cavity energy $\Delta G_{\text{cav}}$.[6]

$$\Delta G_{\text{Sol}} = \Delta G_{\text{el}} + \Delta G_{\text{dis}} + \Delta G_{\text{rep}} + \Delta G_{\text{cav}}. \tag{7}$$

The dispersion and repulsion energy are calculated after a procedure by Floris and Tomasi.[31,32] The

main idea is to use atomic pair potentials and a continuous distribution function of the solvent around the solute. The energy is then calculated in the form of a surface integral.[32] The parameters used in this procedure were taken from the literature[33] except the dispersion coefficients, which were parameterized in this work for a better representation of hydration energies. The atomic radii used in this procedure were determined as the radii of the isodensity surfaces at 0.002 e/Bohr$^3$ of the neutral atoms in the ADM procedure [eq. (8)]. For the cavity energy the well known formula of Pierotti[34] is used. The diameter of the solvent molecules are calculated from the macroscopic density of the solvent. The diameter of the solute is calculated from the surface of the isodensity surface assuming the solute to be spherical with surface $S$.

## Electrostatic Potentials

The calculation of the MESP $V_M(\mathbf{s}_i)$ of the solute molecule is a central problem in the PCM model. The exact calculation of the MESP in the framework of molecular orbital (MO) theory is technically demanding because it requires calculation of a large number of one-, two-, and three-center core attraction integrals. Despite improvements in the algorithm,[35] large systems need an enormous amount of computer time for the calculation of the MESP. To overcome this problem we introduced the ADM[30] as a suitable approximation for the calculation of the MESP. We repeat here briefly the essential idea.

The density of an atom is a monotonically decreasing function of the distance and can be approximated by a superposition of exponential functions.[36] In the ADM the following form is chosen for the density $\rho(r, \vartheta, \varphi)$ of an atom:

$$\rho(r, \vartheta, \varphi) = C_0 e^{-\alpha_0 r} Y_0^0 + \sum_{m=-1}^{1} C_{1m} r e^{-\alpha_{1m} r} Y_1^m. \tag{8}$$

The first exponential function describes the spherical part of the density. The factor $C_0$ is determined by the atomic charge. The other three exponential functions cause a polarization of the atomic density along the Cartesian coordinate axes and allow a description of the anisotropy of the atomic density. The factors $C_{1m}$ are determined by the atomic dipole moments. Equation (8) is inserted into the Poisson equation

$$\nabla^2 V = -4\pi\rho, \tag{9}$$

which is solved for $V$. We obtain a spherical part $V_0^A$ and a nonspherical part $V_1^A$.

$$V_0^A = 4\pi \left[ \frac{1}{r} - \left( \frac{1}{r} + \frac{\alpha_0}{2} \right) e^{-\alpha_0 r} \right] q_0^* Y_0^0, \tag{10}$$

$$V_1^A = \frac{4}{3}\pi \left[ \frac{1}{r^2} - \left( \frac{1}{r^2} + \frac{\alpha_1^3 r}{8} + \frac{\alpha_1^2}{2} + \frac{\alpha_1}{r} \right) e^{-\alpha_1 r} \right] \times \sum_{m=-1}^{1} \mu_m^* Y_1^m, \tag{11}$$

with

$$r = |\mathbf{r}_A - \mathbf{r}|,$$

$$\alpha_0 = \frac{\alpha_0' V_{\text{exact}}^A}{2\pi q_0^* S_0^0},$$

$$q_0^* = \sqrt{\frac{1}{4\pi}}\, q_0^A,$$

$$\mu_m^* = \sqrt{\frac{3}{4\pi}}\, \mu_m^A f_A.$$

$\alpha_0'$, $\alpha_1$ and $f_A$ are atomic parameters (Table I). $V_{\text{exact}}^A$ is the exact electrostatic potential of the underlying wave function at the nucleus. $q_0^A$ is the cumulative atomic charge and $\mu_m^A$ are the cumulative atomic dipole moments. The cumulative atomic multipole moments (CAMM)[37,38] are defined in such a way that the rotational invariance of all moments is conserved. The approximate MESP is finally the sum over the nuclear and electronic potentials of all atoms,

$$V_n(\mathbf{r}) = \sum_A \frac{Z_A}{|\mathbf{R}_A - \mathbf{r}|}, \tag{12}$$

$$V_e(\mathbf{r}) = \sum_A V_0^A(\mathbf{r}) + V_1^A(\mathbf{r}). \tag{13}$$

From these expressions for the MESP analytical derivatives can be easily obtained. Because we

**TABLE I.**
**Atomic Parameters for MESP.**

| Parameter | H | C | N | O | F |
|---|---|---|---|---|---|
| $\alpha_0'$ | 0.70 | 1.30 | 1.90 | 1.60 | 1.20 |
| $\alpha_1$ | 1.00 | 1.20 | 1.40 | 1.00 | 1.10 |
| $f_A$ | 0.80 | 1.00 | 1.30 | 1.40 | 1.60 |
| $g_A$ | 0.60 | 1.25 | 1.11 | 1.00 | 0.97 |

need the derivatives of the MESP with respect to the normal vector $\mathbf{n}_i$, this is an important point. The normal vector is the gradient of the electronic density $\rho$ at this point and can be easily obtained as derivative of eq. (8).

The details of the implementation of the ADM in SINDO1 are described elsewhere.[39] For a better reproduction of the solvation energies the atomic charges used in the ADM had to be modified. Without this modification the solvation energies are too small because the MESP on the cavity surface is too small. This defect was also observed in other semiempirical PCM implementations.[40] In this work each atomic charge $q_0^A$ is scaled with an atomic parameter $g_A$.

$$q_0'^A = g_A q_0^A. \tag{14}$$

The sum of the scaled charges $q_0'^A$ generates an excess charge $\sum_A \Delta q_0^A = \sum_A (q_0^A - q_0'^A)$ for the whole molecule, which must be compensated. This is achieved by a distribution of each atomic excess charge $\Delta q_0^A$ on all other atoms. This distribution is done in a distant dependent way so that the nearest atoms receive the largest part of the excess charge

$$q_0''^I = \frac{\frac{1}{r_I}}{\sum_{J \neq A} \frac{1}{r_J}} \Delta q_0^A + q_0'^I. \tag{15}$$

Here $r_I$ is the distance of atom $I$ to atom $A$ and $q_0'^I$ is the scaled charge on atom $I$. After distribution of the excess charge on the whole molecule, the original total charge is conserved.

## Cavity Surface

An important point for the quality of the PCM results is the definition of the cavity surface. Most implementations use surfaces that are based on the superposition of van der Waals spheres around the atoms of the solute molecule. Besides the simple van der Waals surfaces[41] there are also surfaces generated by a rolling sphere[42,43] and solvent accessible surfaces.[44] All of them have the problem of fixed van der Waals radii independent of the chemical environment of the considered atom, and the van der Waals radii are not unique. To remove the first problem van der Waals radii were made dependent on the atomic charge.[45] To remove the arbitrariness of van der Waals radii one can use them as parameters in semiempirical methods for the optimization of the solvent energies based on PCM calculations.[26,46] A better defined cavity surface is obtained from isodensity surfaces that contain information on the electronic structure of the molecule. In studies of electrostatic potentials on molecular surfaces, density values of 0.001 or 0.002 e/Bohr$^3$ were used.[47,48] In this work we use a density value of 0.002 e/Bohr$^3$. The density values needed for the isodensity surface are calculated after eq. (8) from the ADM so that the density values are consistent with the MESP values. The isodensity surface is calculated with the aid of the marching cube algorithm.[49,50] The marching cube algorithm approximates the surface by a net of triangles with corners of the required density value. According to the PCM model each triangle is assigned a point charge from the center of the triangle. However, this center is not exactly located on the isodensity surface because the surface is curved. Also the sum of triangles does not exactly sum up to the exact surface. To avoid these problems we developed the following procedure. From the center of the triangle we conduct a Newton search along the normal vector of the surface for the point with the exact density. At this point the MESP is calculated in the PCM and the point charge is localized there. This new point and the corners of the triangle define a spherical triangle. The surface size of this spherical triangle can now be easily calculated. The use of this procedure leads to a surface size nearly independent of the resolution of the marching cube algorithm (Figs. 2, 3). This has the advantage that relatively few surface segments suffice to obtain consistent results. In the present work we have chosen 1.5 au as the step size in the marching cube algorithm.

## Hydration Energies

With the model described above the solvation energies of organic molecules in water were calculated. The geometry of the molecules was optimized with the Newton–Raphson procedure implemented for the vacuum. We did not optimize the systems in solution because no significant geometry changes are expected in solution.

The calculated solvation energies together with the major electrostatic components for 16 mostly organic test molecules are compared with experimental data[51] in Table II. In addition results from

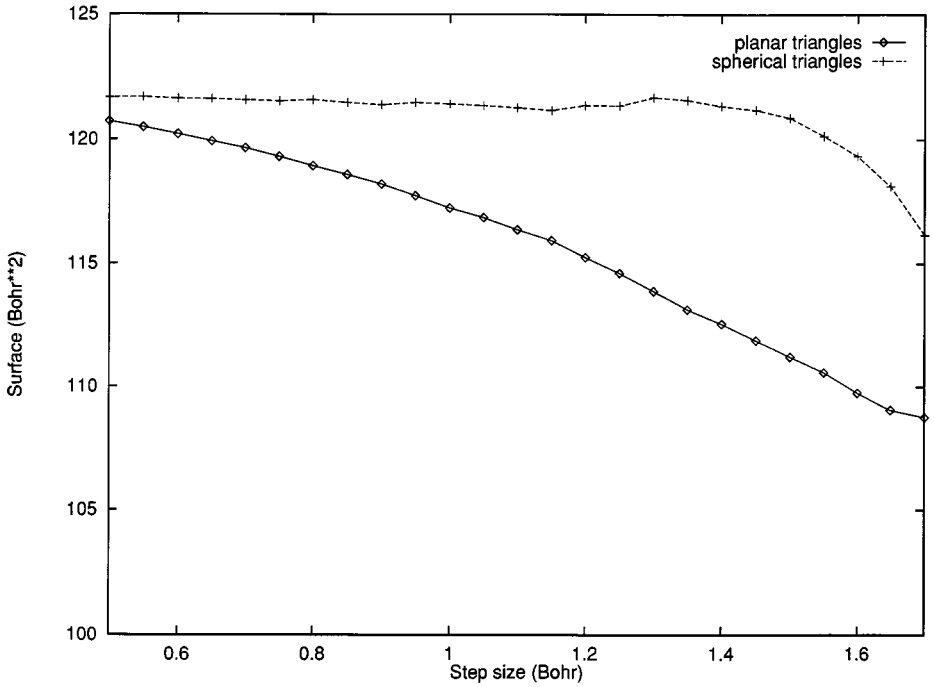


**FIGURE 2.** Surface size (Bohr$^2$) dependent on step size (Bohr) of marching cube algorithm.

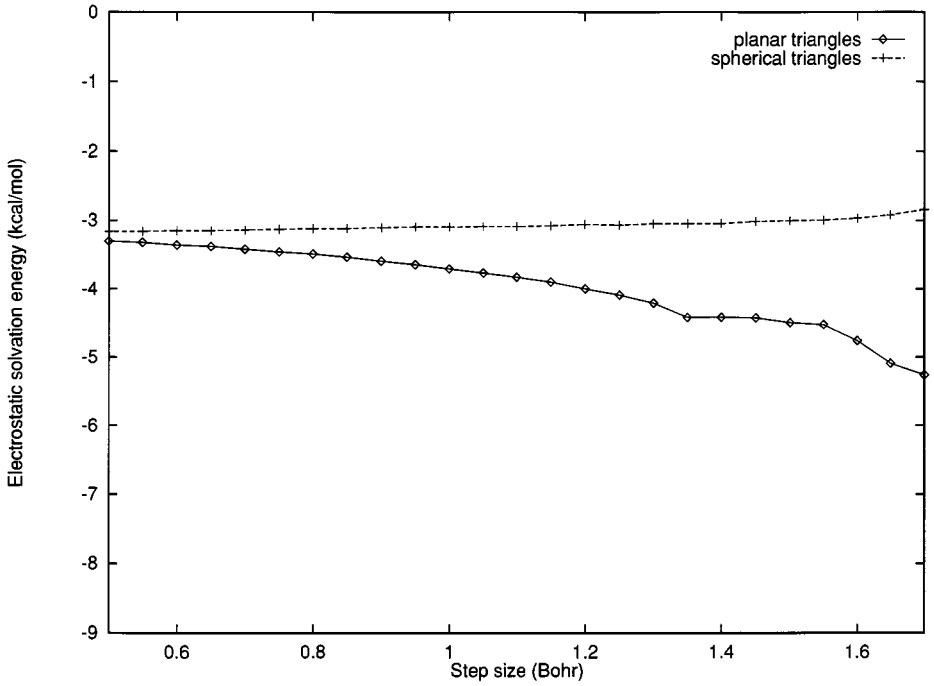


**FIGURE 3.** Electrostatic part of solvation energy (kcal / mol) dependent on step size (Bohr) of marching cube algorithm.

**TABLE II.**
**Comparison of Experimental and Calculated Solvation Energies $\Delta G_{sol}$ (kcal / mol) and SINDO1 Electrostatic Components $\Delta G_{el}$ for Test Molecules.**

| Molecule | $\Delta G_{sol}$ Expt. | AM1 | PM3 | MNDO | SINDO1 | $\Delta G_{el}$ SINDO1 |
|---|---|---|---|---|---|---|
| Methane | 2.00 | 1.22 | 1.44 | 1.41 | 2.05 | −0.18 |
| Ethane | 1.83 | 1.13 | 1.60 | 1.57 | 1.62 | −0.27 |
| Ethene | 1.27 | 0.41 | 0.58 | 0.94 | 1.50 | −0.44 |
| Ethyne | 0.00 | −0.61 | −0.39 | −0.01 | −0.80 | −2.15 |
| Benzene | −0.86 | −1.59 | −1.16 | 0.12 | −1.07 | −1.14 |
| Pyridine | −4.70 | −3.43 | −3.32 | −3.37 | −3.08 | −2.47 |
| Fluoromethane | −0.22 | −0.24 | −0.11 | −1.03 | −0.57 | −2.91 |
| Dimethyl ether | −1.90 | −1.80 | −1.58 | −1.31 | −0.68 | −3.13 |
| Acetone | −3.85 | −3.98 | −4.54 | −3.57 | −4.40 | −5.99 |
| Acetaldehyde | −3.50 | −3.45 | −3.67 | −3.49 | −2.64 | −4.57 |
| Acetic acid methyl ester | −3.31 | −3.78 | −3.91 | −4.33 | −4.22 | −6.21 |
| Ammonia | −4.30 | −4.69 | −3.14 | −4.57 | −3.80 | −2.51 |
| Methylamine | −4.57 | −3.82 | −2.91 | −3.41 | −2.71 | −2.87 |
| Acetic acid | −6.71 | −6.05 | −5.67 | −7.20 | −5.64 | −7.05 |
| Acetamide | −9.72 | −9.59 | −9.67 | −8.96 | −10.08 | −9.06 |
| Phenol | −6.62 | −4.60 | −3.76 | −3.61 | −6.89 | −6.59 |

the other semiempirical methods AM1, PM3, and MNDO[46] are presented. In the latter work the electrostatic potentials needed for the PCM are calculated with two different procedures from semiempirical wave functions. The values in Table II are calculated with MESP values from orthogonal wave functions using the NDDO approximation for three-center integrals. The root mean square deviation from the experiments for these 16 compounds is 0.86 kcal/mol compared to 0.78 kcal/mol for AM1, 1.04 kcal/mol for PM3, and 1.02 kcal/mol for MNDO. For a larger number of selected organic compounds the deviation for SINDO1 is 0.69 kcal/mol. The detailed results are in Table III and Figure 4. We did not include aliphatic alcohols. Here the solvation energies are significantly too small in SINDO1. The reason is that the PCM does not account for the hydrogen bonds between the alcohol and water molecules. In PCM implementations based on van der Waals surfaces or related procedures for cavity surfaces mentioned earlier, this effect is compensated by a choice of reduced van der Waals radii (0.8 Å) for hydrogen atoms bound to heteroatoms compared to normal van der Waals radii (1.2–1.3 Å) for hydrogen bound to carbon. This leads to more positive MESP values in the region of the hydrogen atoms due to the smaller distance to the nucleus and consequently to larger electrostatic interaction energies. This effect cannot be achieved

**TABLE III.**
**Comparison of Experimental and SINDO1 Solvation Energies $\Delta G_{sol}$ (kcal / mol) and SINDO1 Electrostatic Component $\Delta G_{el}$.**

| Molecule | $\Delta G_{sol}$ Expt. | SINDO1 | $\Delta G_{el}$ SINDO1 |
|---|---|---|---|
| Formic acid methyl ester | −2.78 | −2.53 | −4.93 |
| Formic acid ethyl ester | −2.64 | −2.80 | −5.31 |
| Propane | 1.95 | 2.09 | 0.07 |
| Toluene | −0.88 | −1.29 | −1.93 |
| Butane | 2.08 | 2.12 | 0.00 |
| Naphthalene | −2.39 | −2.62 | −1.79 |
| Acetophenone | −4.58 | −3.51 | −3.74 |
| 4-Heptanone | −2.95 | −2.92 | −5.61 |
| 2-Heptanone | −3.04 | −3.71 | −6.54 |
| 2-Pentanone | −3.53 | −3.44 | −5.73 |
| 2-Hexanone | −3.29 | −3.60 | −6.08 |
| 2-Octanone | −2.88 | −4.00 | −7.02 |
| Pentanal | −3.03 | −3.00 | −5.77 |
| Propanal | −3.44 | −3.85 | −5.76 |
| Butanal | −3.18 | −2.79 | −4.99 |
| Cyclopentane | 0.56 | 0.40 | −0.64 |
| Trifluoromethane | 0.81 | 0.44 | −1.66 |
| Tetrafluoromethane | 3.11 | 2.00 | −0.08 |
| Tetrafluoroethene | 1.37 | 0.96 | 0.01 |

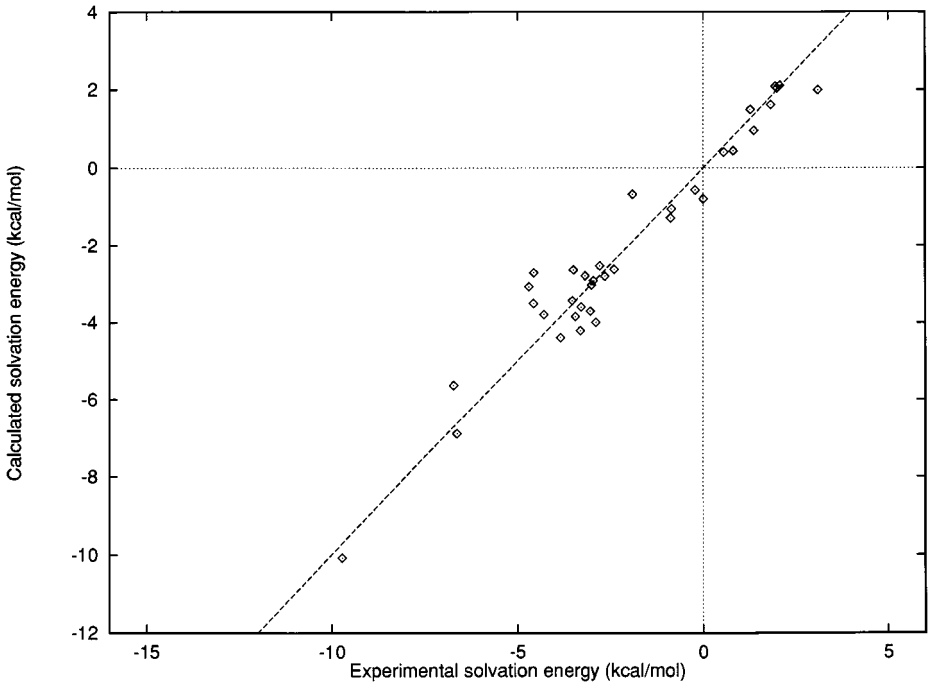


**FIGURE 4.** Comparison of experimental and SINDO1 solvation energies (kcal / mol).

with isodensity surfaces. Too small solvation energies are also to be expected for other solutes with hydrogen bonds, e.g., methylamine, but not so pronounced as for aliphatic alcohols.

For alkanes the electrostatic part of the solvation energy plays only a minor role. Here the cavity energy is dominant. The good results for these compounds show that the simple model with the Pierotti formula suffices to describe this part. Finally it should be emphasized that the quality of the wave function is decisive for the quality of the calculated solvation energy.

## Conclusion

The PCM has proved to be an effective method for the calculation of electrostatic solvation energies. The use of semiempirical MO methods allows the calculation of larger systems. The implementation of the PCM in SINDO1 was greatly enhanced by the use of the ADM because it results in a great reduction in computer time for the MESP compared to the standard methods. Therefore the computer time determining step with the ADM approximation is no longer the calculation of the MESP on the cavity surface, but the iterative determination of the surface charges. Another advantage is the use of isodensity surfaces that provide a physical means of accounting for the chemical environment. Short-range chemical interactions, e.g., hydrogen bonds, cannot be accounted for in the electrostatic model.

The combination of the PCM, the ADM for the MESP, and the isodensity surfaces in SINDO1 opens new possibilities to describe the influence of solvents on systems not accessible to *ab initio* methods and systems too difficult for other semiempirical methods that use a standard procedure for the MESP.

## Acknowledgments

C. K. thanks J. Madrileijos for a part of the calculations. The calculations were performed on two DEC-Alpha 300 workstations, one of them from the Institut für Makromolekulare Chemie. We thank Deutsche Forschungsgemeinschaft and Deutscher Akademischer Austauschdienst for partial financial support.

## References

1. J. Tomasi and M. Persico, *Chem. Rev.*, **94**, 2027 (1994).
2. J. P. Valleau and S. G. Whittington, In *Statistical Mechanics Part A*, B. J. Berne, Ed., Plenum Press, New York, 1977, p. 137.

3. J. P. Valleau and G. M. Torrie, In *Statistical Mechanics Part A*, B. J. Berne, Ed., Plenum Press, New York, 1977, p. 169.
4. J. Kushick and B. J. Berne, In *Statistical Mechanics Part B*, B. J. Berne, Ed., Plenum Press, New York, 1977, p. 41.
5. J. Tomasi, G. Alagona, R. Bonaccorsi, and C. Ghio, In *Modelling of Structure and Properties of Molecules*, Z. B. Maksic, Ed., Ellis Horwood, Chichester, 1987, p. 330.
6. R. Bonaccorsi, F. Floris, P. Palla, and J. Tomasi, *Thermochim. Acta*, **162**, 213 (1990).
7. G. P. Ford and B. Wang, *J. Am. Chem. Soc.*, **114**, 10563 (1992).
8. T. Furuki, M. Sakurai, Y. Inoue, R. Chujo, and K. Harata, *Chem. Phys. Lett.*, **188**, 584 (1992).
9. M. Orozco, W. L. Jorgensen, and F. J. Luque, *J. Comput. Chem.*, **14**, 1498 (1993).
10. C. J. Cramer and D. G. Truhlar, *J. Am. Chem. Soc.*, **113**, 8305 (1991).
11. G. Alagona, R. Bonaccorsi, C. Ghio, and J. Tomasi, *J. Mol. Struct.: Theochem*, **137**, 263 (1986).
12. K. B. Wibert and M. W. Wong, *J. Am. Chem. Soc.*, **115**, 1078 (1993).
13. R. R. Pappalardo, E. Sanchez Marcos, M. F. Ruiz−Lopez, D. Rinaldi, and J.-L. Rivail, *J. Phys. Org. Chem.*, **4**, 141 (1991).
14. R. Bonaccorsi, R. Cimiraglia, and J. Tomasi, *J. Comput. Chem.*, **4**, 567 (1983).
15. R. Bonaccorsi, R. Cimiraglia, and J. Tomasi, *Chem. Phys. Lett.*, **99**, 77 (1983).
16. M. M. Karelson and M. C. Zerner, *J. Phys. Chem.*, **96**, 6949 (1992).
17. T. Fox and N. Rösch, *J. Mol. Struct.: Theochem*, **276**, 279 (1992).
18. R. Bianco, S. Miertus, M. Persico, and J. Tomasi, *Chem. Phys.*, **168**, 281 (1992).
19. M. Aguilar, R. Bianco, S. Miertus, M. Persico, and J. Tomasi, *Chem. Phys.*, **174**, 397 (1993).
20. C. J. F. Böttcher, *Theory of Electric Polarization*, vol. 1, Elsevier, Amsterdam, 1973.
21. D. Rinaldi and J.-L. Rivail, *Theor. Chim. Acta*, **32**, 57 (1973).
22. O. Tapia and O. Goscinski, *Mol. Phys.*, **29**, 1653 (1975).
23. M. W. Wong, M. J. Frisch, and K. B. Wiberg, *J. Am. Chem. Soc.*, **113**, 4776 (1991).
24. S. Miertus, E. Scrocco, and J. Tomasi, *Chem. Phys.*, **55**, 117 (1981).
25. G. Rauhut, T. Clark, and T. Steinke, *J. Am. Chem. Soc.*, **115**, 9174 (1993).
26. F. J. Luque, M. Bachs, and M. Orozco, *J. Comput. Chem.*, **15**, 847 (1994).
27. D. N. Nanda and K. Jug, *Theor. Chim. Acta*, **57**, 95 (1980).
28. K. Jug, R. Iffert, and J. Schulz, *Int. J. Quantum Chem.*, **32**, 265 (1987).
29. J. Li, P. Correa de Mello, and K. Jug, *J. Comput. Chem.*, **13**, 85 (1992).
30. A. M. Köster, C. Kölle, and K. Jug, *J. Chem. Phys.*, **99**, 1224 (1993).
31. F. Floris and J. Tomasi, *J. Comput. Chem.*, **10**, 616 (1989).
32. F. M. Floris, J. Tomasi, and J. L. Pascual Ahuir, *J. Comput. Chem.*, **12**, 784 (1991).
33. F. Vigné−Maeder and P. Claverie, *J. Am. Chem. Soc.*, **109**, 24 (1987).
34. R. A. Pierotti, *Chem. Rev.*, **76**, 717 (1976).
35. B. G. Johnson, P. M. W. Gill, J. A. Pople, and D. J. Fox, *Chem. Phys. Lett.*, **206**, 239 (1993).
36. W. P. Wang and R. G. Parr, *Phys. Rev. A*, **16**, 891 (1977).
37. W. A. Sokalski and R. A. Poirier, *Chem. Phys. Lett.*, **98**, 86 (1983).
38. W. A. Sokalski, M. Shibata, R. L. Ornstein, and R. Rein, *J. Comput. Chem.*, **13**, 883 (1992).
39. M. Krack, A. M. Köster, and K. Jug, *J. Comput. Chem.*, to appear.
40. C. Aleman, F. J. Luque, and M. Orozco, *J. Comput.-Aid. Mol. Design*, **7**, 721 (1993).
41. J. L. Pascual−Ahuir, E. Silla, J. Tomasi, and R. Bonaccorsi, *J. Comput. Chem.*, **8**, 778 (1987).
42. F. M. Richards, *Annu. Rev. Biophys. Bioeng.*, **6**, 151 (1977).
43. J. L. Pascual−Ahuir, E. Silla, and I. Tunon, *J. Comput. Chem.*, **15**, 1127 (1994).
44. B. Lee and F. M. Richards, *J. Mol. Biol.*, **55**, 379 (1971).
45. M. A. Aguilar and F. J. Olivares del Valle, *Chem. Phys.*, **129**, 439 (1989).
46. M. Orozco, M. Bachs, and F. J. Luque, *J. Comput. Chem.*, **16**, 563 (1995).
47. J. S. Murray and P. Politzer, *Theor. Chim. Acta*, **72**, 507 (1987).
48. T. Brinck, J. S. Murray, and P. Politzer, *Int. J. Quantum Chem.: Quantum Biol. Symp.*, **19**, 57 (1992).
49. W. E. Lorensen and H. E. Cline, *Comput. Graphics*, **21**, 163 (1987).
50. W. Heiden, T. Goetze, and J. Brickmann, *J. Comp. Chem.*, **14**, 246 (1993).
51. S. Cabani, P. Giani, V. Mollica, and L. Lepora, *J. Solut. Chem.*, **10**, 563 (1981).